Research Article

Mohammad Azam Ansari*, Hassan Nassr Al Dhneem#, Syed Ghazanfar Ali#, Yahya Fahad Jamous, Mohammad Nasser Alomary, Banan Atwah, Maryam Saleh Alhumaidi, Umme Hani, Nazima Haider, Sarah Asiri, and Firdos Alam Khan

Facile, polyherbal drug-mediated green synthesis of CuO nanoparticles and their potent biological applications

https://doi.org/10.1515/gps-2023-0174
received September 11, 2023; accepted January 7, 2024

Abstract: Copper oxide nanoparticles (CuO NPs) were synthesized using ayurvedic medicine septilin. The septilin-mediated CuO NPs were characterized using UV–Vis, fourier-transform infrared spectroscopy, X-ray diffraction (XRD), scanning electron microscope (SEM), and transmission electron microscope (TEM). The average particle size of CuO NPs was 8 nm as evident from TEM. Minimum inhibitory concentration of CuO NPs against *Escherichia coli*, *Pseudomonas aeruginosa*, methicillin-resistant *Staphylococcus aureus* (MRSA), and *Candida albicans* was found in the range of 1–2.5 mg·mL^{-1}. CuO NPs dose-dependently decreased the biofilm formation from 0.0315 to 2 mg·mL^{-1}, at the highest dose of 2 mg·mL^{-1} of CuO NPs; 92.91%, 79.84%, and 71.57% decrease in biofilm was observed for *P. aeruginosa*, MRSA, and *C. albicans*, respectively. Down-regulation of biofilm upon treatment with nanoparticles (NPs) was also observed by SEM analysis. SEM analysis also showed the change in morphological structure, and deformities in bacterial and fungal cells upon treatment of NPs. Furthermore, the anticancer efficacy of NPs was assessed using colon cancer (HCT-116). The 3-(4,5-dimethylthiazol-2-yl)-2,5-diphenyltetrazolium bromide assay clearly showed the anticancer potential of NPs, as the concentration of CuO NPs increased, the number of viable cells decreased. The produced CuO NPs have promise for future investigations in many biological and therapeutic domains, including the treatment of microbial biofilm infections, as well as the inhibition of cancer cell growth.

Keywords: *C. albicans*, CuO NPs, multi-drug resistance, biofilm, colon cancer, polyherbal drug

1 Introduction

The multi-drug resistance (MDR) can be defined in a simpler form as the resistance developed by the microorganism against the lethal doses of antimicrobials. The MDR developed by microorganisms has become a health concern, specifically against pathogenic diseases [1]. The ineffectiveness of antimicrobials against MDR has risen many folds during the last few years, several reports have warned that MDR is a considerable risk to human health in European countries [2]. According to data from

# These authors are contributed equally.

*** Corresponding author: Mohammad Azam Ansari**, Department of Epidemic Disease Research, Institute for Research and Medical Consultations (IRMC), Imam Abdulrahman Bin Faisal University, 31441, Dammam, Saudi Arabia, e-mail: maansari@iau.edusa
Hassan Nassr Al Dhneem: Department of Internal Medicine, King Fahd Hospital of the University, Imam Abdulrahman Bin Faisal University, 31441, Dammam, Saudi Arabia
Syed Ghazanfar Ali: Department of Microbiology, Jawaharlal Nehru Medical College, Aligarh Muslim University, Aligarh, U.P., India
Yahya Fahad Jamous: Vaccine and Bioprocessing Center, King Abdulaziz City for Science and Technology (KACST), Riyadh, 11442, Saudi Arabia
Mohammad Nasser Alomary: Advanced Diagnostic and Therapeutic Institute, King Abdulaziz City for Science and Technology (KACST), Riyadh, 11442, Saudi Arabia
Banan Atwah: Clinical Laboratory Sciences Department, College of Applied Medical Sciences, Umm Al-Qura University, Makkah, Kingdom of Saudi Arabia
Maryam Saleh Alhumaidi: Department of Biology, College of Science, University of Hafr Al Batin, P.O. Box 1803, Hafr Al Batin, 31991, Saudi Arabia
Umme Hani: Department of Pharmaceutics, Collage of Pharmacy, King Khalid University, Abha, Saudi Arabia
Nazima Haider: Department of Pathology, College of Medicine, King Khalid University, Abha, Saudi Arabia
Sarah Asiri: Department of Biophysics, Institute for Research and Medical Consultations (IRMC), Imam Abdulrahman Bin Faisal University, P.O. Box: 1982, Dammam, 31441, Saudi Arabia
Firdos Alam Khan: Department of Stem Cell Biology, Institute for Research and Medical Consultations, Imam Abdulrahman Bin Faisal University, Post Box No. 1982, Dammam, 31441, Saudi Arabia

the United States, the additional societal and healthcare costs associated with MDR diseases are estimated to 55 billion dollars per year [3]. The delay in developing new antimicrobial agents further worsens the situation [4]. The data collected from the different hospitals in the United States reports 40–60% of *Staphylococcus aureus* strains to be methicillin resistant and, in some cases, even vancomycin and carbapenem resistant [5].

Biofilms are the communities of microorganism that are complex and attach to the surface or substratum. These complex communities are enclosed in a self-polymer matrix which is composed of polysaccharide, proteins, and DNA [6]. The formation of biofilm by microorganisms is one of the adaptive features to survive in harsh environmental conditions [7]. The biofilm provides a better adaptive environment for survival compared to the planktonic cells, which includes a stronger ability to grow in an oligotrophic environment [8], and provides better nutrition [9] and improved organism productivity and their interactions [10].

Colon cancer, also called colorectal cancer (HCT-116), is one of the most common cancers in developing and developed nations [11,12]. Colorectal cancer is the third most cancer in the category of malignant tumors occurring in humans, and the mortality rate is increasing globally with a decrease in survival rate [13]. Treatment of colorectal cancer is still an unsolved issue, but for the sake of treatment, the only option left is chemotherapy [14].

Nanotechnology in today's world is not only confined to the electronics but also has shown promising results in biomedical, pharmaceutical, and environmental sciences [15]. Due to the involvement of nanotechnology in different aspects, it is believed that it can also play a key role in the improvement of human health [16]. Nanoparticles (NPs) can be produced via physical, chemical, or biological processes. A few drawbacks of physical and chemical processes are that they need high temperatures, while chemical methods need hazardous chemicals [17]. Biological method is the most preferred method since it is safer, cheaper, and nonhazardous and does not involve any toxic product [18,19]. Green route of NP synthesis has been used for different NPs, including silver [20], gold [21], platinum [22], and zinc [23]. The results from gold, silver, and platinum in terms of antimicrobial and antibiofilm are promising, but when it is compared with copper, it is cheaper and more effective than gold and silver [24]. Due to the easy availability of copper and being antimicrobial in nature, the copper oxide nanoparticles (CuO NPs) are gaining attention [25].

The use of nanomaterials in medicine is not new; it has been in practice since ancient times. Ayurveda is a traditional system of medicine that has been practiced in India for seven centuries. In ancient times, people used metal ash, which is also called Bhasma, to treat different diseases [26]. Septilin is one of the ayurvedic drugs manufactured by Himalayan Drug Company (India), which contains extracts of several ayurvedic plants. Septilin drug has been extensively used in severe acute and chronic infections due to its antibacterial, anti-inflammatory, immunomodulatory, and immunopotentiating effects [27,28]. Keeping in view the importance of green synthesis of NPs, we have synthesized CuO NPs from the ayurvedic drug septilin and tested them for their potential pharmaceutical and medical applications, such as antimicrobial, antibiofilm, and anticancer.

2 Materials and methods

2.1 Preparation of septilin aqueous extract

Ayurvedic herbal medicine septilin (manufactured by Himalaya Company) was purchased from the local market. Few tablets (drugs) were taken and ground into the fine powder using mortar and pestle and passed through the muslin cloth. A rotary shaker was used for mixing 10 g of powdered septilin with 90 mL of sterile water for 30 min at 60 rpm. After that, the extract was filtered and preserved for subsequent use at 4°C.

2.2 Septilin-mediated biosynthesis of CuO NPs

Ten milliliters of septilin extract was added to 90 mL of copper nitrate solution. The solution was subsequently left on the stirrer for 24 h, after which an apparent change in color was seen.

2.3 Characterization techniques

The septilin-mediated NPs were scanned using UV-Vis Spectrophotometer (UV-Vis) at the wavelength of 230–330 nm. Fourier-transform infrared spectroscopy (FTIR) was performed in the range of 4,000–500 cm^{-1} at room temperature. FTIR has been used to identify the functional groups that are present in the synthesized CuO NPs. It utilizes the energy absorption bands associated with each chemical bond to determine the structural and bonding information of the complex. This allows for the identification of the bonding type and strength of the

bond. To know the morphology and size of NPs, scanning electron microscope (SEM) and transmission electron microscope (TEM) were performed by the method previously described [29]. X-ray diffraction (XRD) (Rigaku, Pittsburg, PA, USA) analysis was performed to know the nature of NPs, whether amorphous or crystalline at 2θ ranges from 20° to 70° at 40 keV.

2.4 Determination of minimum inhibitory concentration (MIC)

MIC of green-synthesized CuO NPs was determined using the microbroth dilution method previously described [30]. The bacterial strains, i.e., *Escherichia coli*, MDR-*Pseudomonas aeruginosa* (MDR-PA), methicillin-resistant *S. aureus* (MRSA), and *Candida albicans* cultures, were treated to two-fold serial dilutions of CuO NPs and then incubated at a 37°C for 24 h. The MIC was tested using the brain heart infusion broth. The MIC value refers to the initial concentration of NPs at which no observable growth is detected [30].

2.5 Antibiofilm using crystal violet assay

The antibiofilm potential of NPs was evaluated using the method previously described [30]. Briefly, 100 µL of mid-exponential culture of bacteria and fungus were incubated in a 96-well culture plates at 37 and 28°C for 24 h in a shaking incubator with or without CuO NPs. The wells were washed and 0.1% w/v crystal violet was added in each well for 30 min. After further washing, wells were filled with ethanol, and optical density was recorded at 595 nm.

$$\text{Percent inhibition of biofilm} = \frac{1 - \text{Absorbance of cells treated with nanoparticles}}{\text{Absorbance of untreated cells}} \times 100$$

2.6 SEM analysis of interaction of CuO NPs with bacterial/fungal cells

The interaction of bacterial and fungal cells was observed using SEM as previously described [31]. Briefly, the overnight-grown bacterial and fungal cells were treated with CuO NPs and then incubated for 16 h at 37°C. After the period of incubation, the samples underwent centrifugation for a duration of 15 min. The resulting pellets were subsequently subjected to four rounds of washing using PBS. Following a fixation step using 2.5% glutaraldehyde and 1% osmium tetroxide, it was dehydrated with 20, 30, 40, 50, 60, 70, 80, 90, and 100% ethanol. Subsequently, the samples were placed onto the aluminum stubs and then coated with gold. The impact of NPs on the structure of tested pathogens was examined using an SEM operating at 20 kV [30].

3 Cytotoxicity analysis

3.1 Anticancer activity

Cell proliferation test was used to examine the impact of different concentrations of NPs on colon cancer cell viability using 3-(4,5-dimethylthiazol-2-yl)-2,5-diphenyltetrazolium bromide (MTT) assay as the method described in our previous study [30]. In brief, the cells were cultured at 37°C in dulbecco's modified eagle medium with 1% penicillin–streptomycin, 1% L-glutamine, and 10% fetal bovine serum. The culture was maintained in a humid room with a 5% CO_2 atmosphere. The cells were subsequently treated to a concentration range of 11–118 $\mu g \cdot mL^{-1}$ of NPs for a duration of 48 h, after which they were prepared for the cell viability experiment. No NPs were added to the untreated control. Following 4 h of MTT (5.0 $mg \cdot mL^{-1}$) incubation, cell viability was calculated at 570 nm using the below formula:

$$\text{Cell viability (\%)} = \text{OD of sample/OD of control} \times 100$$

3.2 Microscopic analysis

Under an inverted microscope, the structural morphology of HCT-116 cells was examined. In brief, HCT-116 cells were exposed to different doses of CuO NPs and then incubated for a duration of 48 h. Following a 48-hour treatment period, the cells were rinsed and the impact of NPs on the morphology and cellular proliferation of HCT-116 was assessed by observing them under an inverted microscope.

4 Result

4.1 Synthesis and characterization of CuO NPs

The schematic illustration (Figure 1) shows the formation of CuO NPs from the drug septilin. UV–Vis spectra show the intense peak at 285 nm, which is due to the surface plasmon resonance (Figure 2). FTIR spectra showed

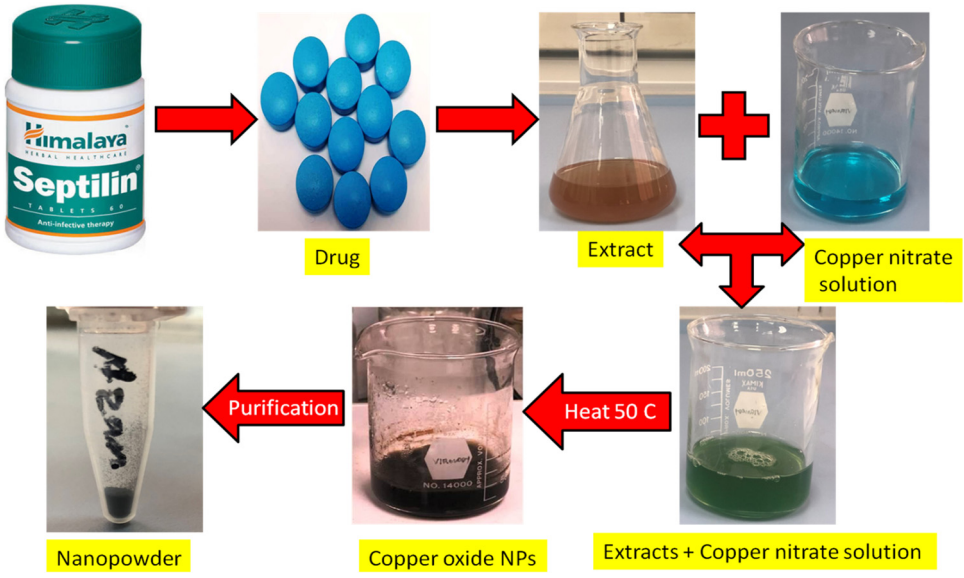

Figure1: Scheme of green synthesis of CuO NPs.

various peaks at 3,243, 2,925, 1,697, 1,576, 1,325, 1,019, 730, and 517, which corresponds to OH stretching, C–H asymmetric, C═C stretching, C═C stretching, OH bending, C–OH bending, C═C bending, and halo compounds, respectively (Figure 3). The XRD peaks of CuO NPs were located at 2θ = 32.2°, 35.2°, 38.8°, 48.6°, 53.2°, 57.8°, 61.3°, and 67.8° mainly attributed to the (110), (002), (111), (202), (020), (202), (113), and (220) planes, respectively, that represent the monoclinic structure of CuO NPs (Figure 4) The crystalline size calculated was 10.88 nm. SEM represents the surface morphology (Figure 5a), and it shows that the NPs formed are segregated not clumped, although the better picture is represented by TEM (Figure 5b), where the individual NPs can be more clearly seen and average size was found 8 nm (Figure 5c).

5 Antimicrobial activity

5.1 MIC

MIC for gram-negative *E. coli* and MDR-PA accounts for 2.5 mg·mL^{-1}, whereas the MIC for gram-positive MRSA was 1 mg·mL^{-1} and it was 2.5 mg·mL^{-1} for *C. albicans*.

5.2 Antibiofilm activity

Inhibition of biofilm was observed at all the tested concentrations. The decrease in biofilm for *P. aeruginosa* ranged from 28.47% to 92.91%. At the lowest dose, i.e., 0.0315 mg·mL^{-1}, a 28.47% decrease in biofilm was observed, whereas at the highest dose, i.e., 2 mg·mL^{-1}, the maximum reduction of 92.91% in biofilm was observed. Similarly, a 24.8–79.84% decrease in biofilm was observed for MRSA. The lowest concentration of CuO NPs (0.0315 mg·mL^{-1}) decreased the biofilm by 24.8% and, at 2 mg·mL^{-1} of CuO NPs, the maximum decrease of 79.84% was observed. For *C. albicans* decrease in biofilm ranged from 16.45% to 71.57%. At the lowest concentration of CuO NPs (0.0315 mg·mL^{-1}), a 16.45% decrease was observed, whereas a 71.5% decrease in biofilm was observed at 2 mg·mL^{-1} of CuO NPs (Figure 6).

5.3 Interaction of bacterial/fungal cells

SEM analysis revealed the microscopic changes in *P. aeruginosa*, MRSA, and *C. albicans* upon treatment with CuO

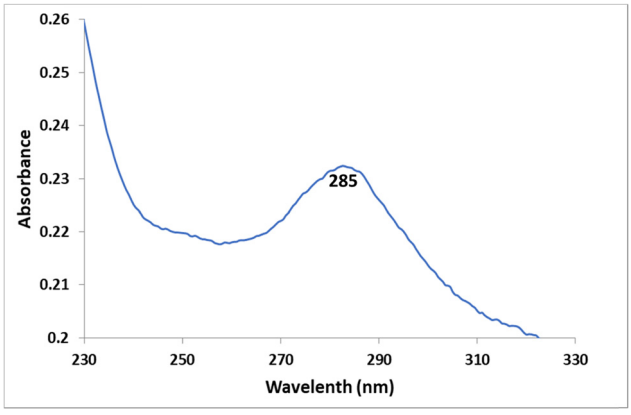

Figure 2: UV–Vis spectra of green-synthesized CuO NPs.

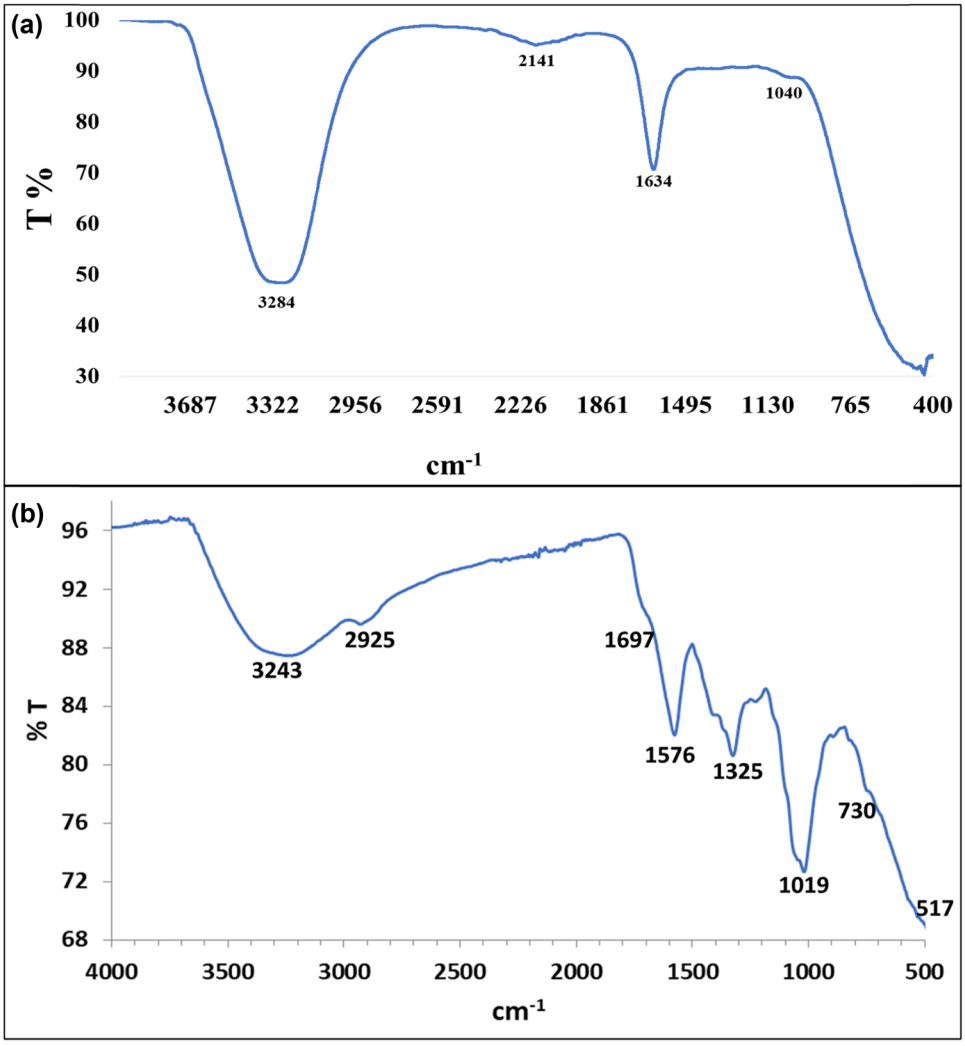

Figure 3: FTIR spectra of herbal drug extract (a) and green-synthesized CuO NPs (b).

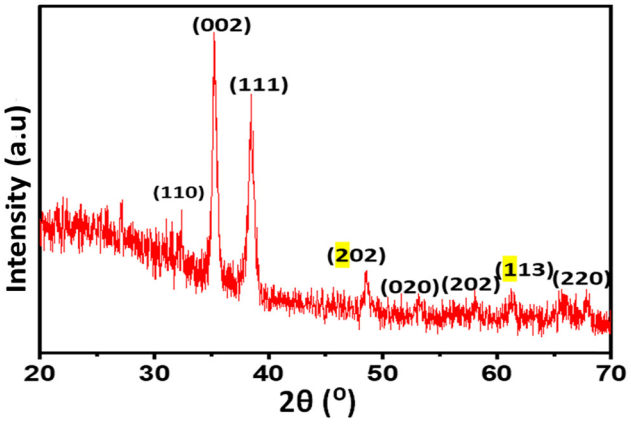

Figure 4: XRD pattern of as-prepared CuO NPs.

NPs. SEM images are indicative of structural changes in cells. Figure 7(a–c) shows the normal morphology of *P. aeruginosa*, MRSA, and *C. albicans*. In contrast, treated cells Figure 7(a1–c1) shows the destruction in cell morphology, shrinkage in cell size, and distorted cell structures.

5.4 Anticancer potential of CuO NPs

A statistical decrease in cell viability (HCT-116 cell line) was observed upon treatment with CuO NPs at all tested concentrations as revealed by MTT (Figure 8). At 11.80 $\mu g \cdot mL^{-1}$ of NPs, 80.62% of cells were viable, whereas at 23.60 $\mu g \cdot mL^{-1}$, only 60% of cells were viable. Furthermore, an increase in CuO NPs to 59.0 $\mu g \cdot mL^{-1}$ down-regulated the viability, and only 37.03% of cells remain viable, and at the highest dose, i.e., 118 $\mu g \cdot mL^{-1}$, the maximum decrease in viability was observed and only 10.15% of cells remain viable (Figure 9).

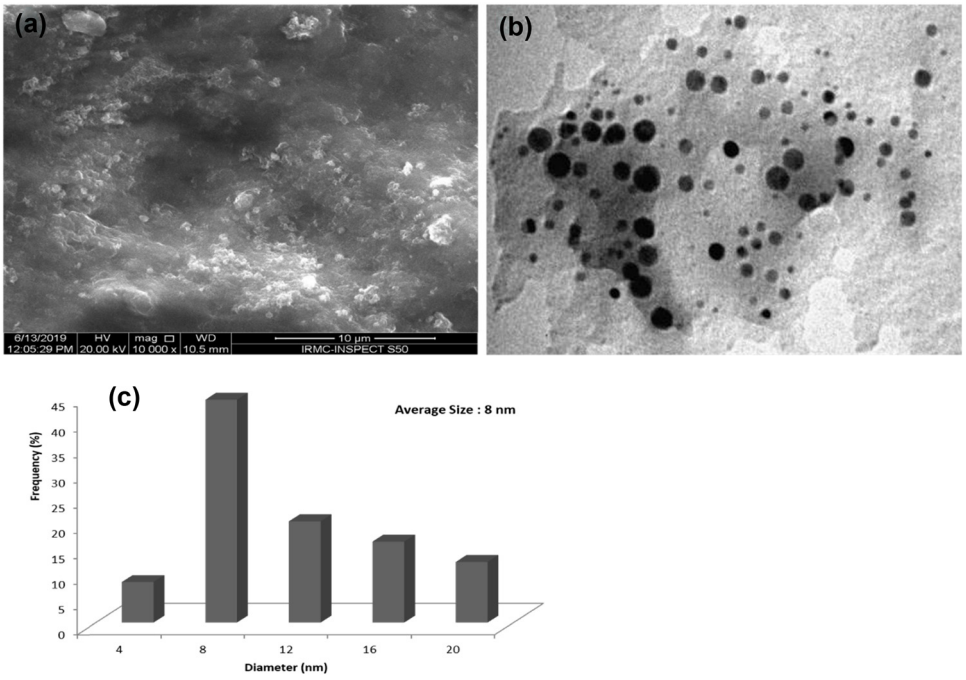

Figure 5: SEM (a), TEM, (b), and histogram (c) analysis.

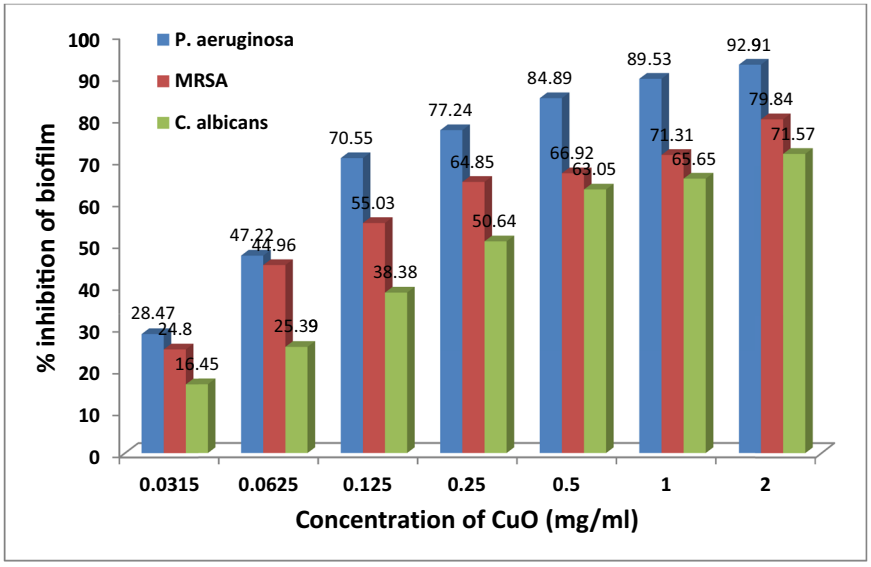

Figure 6: Effects of CuO NPs on biofilm-forming abilities of tested pathogens.

6 Discussion

The color change of septilin extract + copper nitrate solution was the initial sign of NP formation, which was further confirmed by the UV–Vis (Figure 1). The strong peaks detected at a wavelength of 285 nm are similar to the ultraviolet range of CuO NPs (Figure 2). An identical absorbance peak at a wavelength of 290 nm was observed for the CuO NPs that were produced through green method [32]. The UV spectra results align with prior studies that have reported absorption peaks at around 250 and 272 nm for CuO NPs produced from *Caesalpinia bonducella* [33] and *Ephedra alata* [34] extracts, respectively. The highest absorbance peak of CuO NPs is influenced by various factors, including temperature, type precursor salts and plant extract, and the synthesis method used. However, values as low as 219–500 nm have

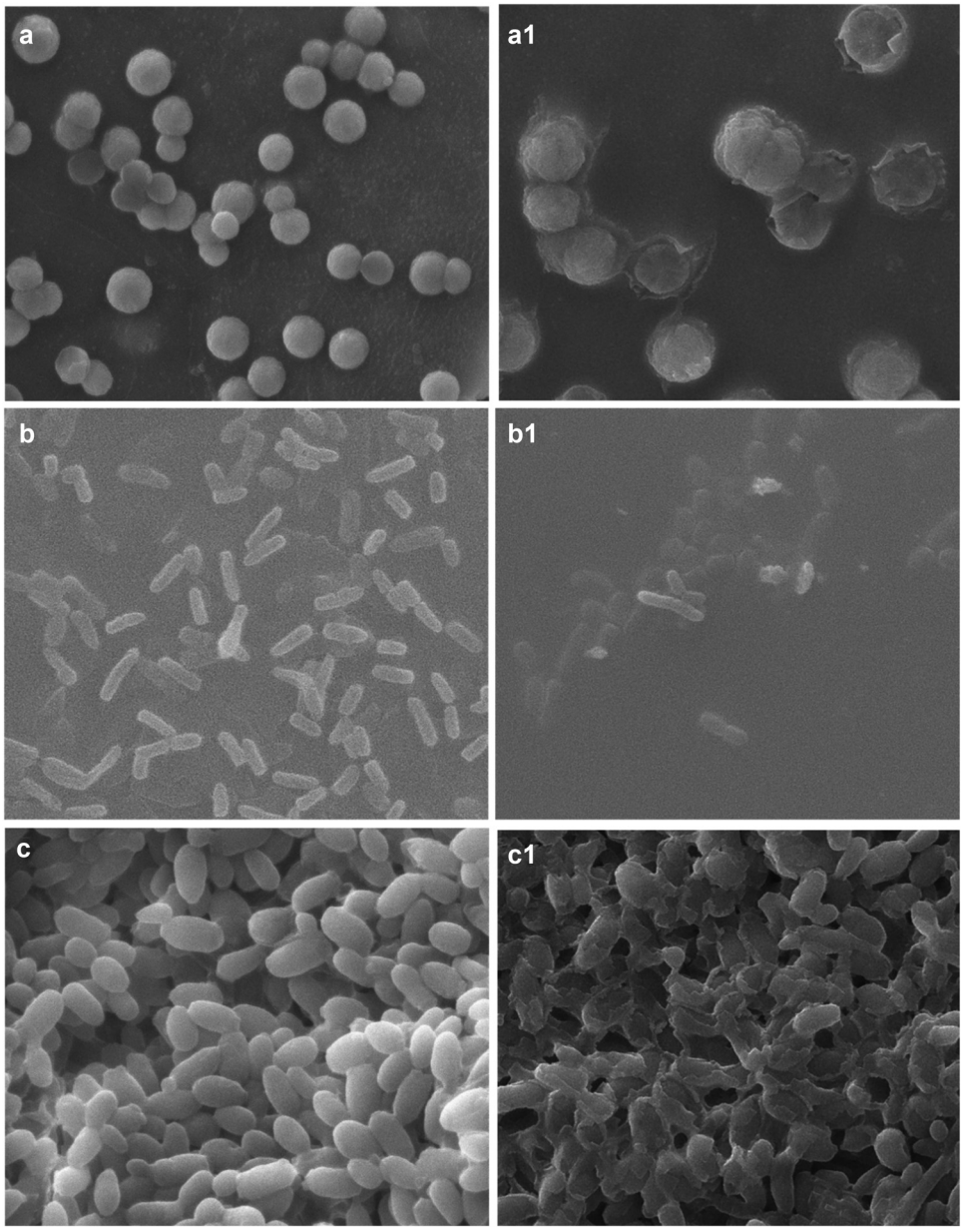

Figure 7: SEM analysis. (a) MRSA control and (a1) treated MRSA; (b) *P. aeruginosa* control and (b1) treated; and (c) *C. albicans* control and (c1) treated.

been documented for CuO NPs in the literature [35]. The medicinal extract from the septlin drug may function as a capping, reducer, and stabilizer agent, reducing copper nitrate into CuO NPs. FTIR analysis was conducted to locate the stretching and vibrating bonds in biosynthesized NPs and to locate the biomolecules present in the septilin extract that may act as reducing and capping agents (Figure 3). The peak at 3,284 cm^{-1} in extract (Figure 3a) and 3,243 cm^{-1} (Figure 3b) of green-synthesized CuO NPs correlates to the vibrational frequency of O–H stretching [35], whereas the peak in the herbal extract at 1,634 cm^{-1} indicates the C═O stretching of acids or ketones [33]. The spectral peaks seen at 2,925 cm^{-1} correspond to the stretching of C–H bonds [34]. The prominent peaks observed at 1,325, 1,576, and 1,697 cm^{-1} correspond to the bending of phenolic O–H bonds and the stretching of C═O bonds in ketones [35,36]. The peaks at 1,019 and 730 cm^{-1} corresponds C–O and C–H bonds, respectively [37]. The peaks at 517 cm^{-1} suggest the formation of a CuO nanostructure and the existence of Cu–O stretching [35,37]. The FTIR spectrum provides evidence that the plant extract contained carboxylic acid, carbohydrates, flavonoids, phenols, and alkaloids. These compounds facilitated the synthesis of NPs and functioned as capping and stabilizing agents [34,36].

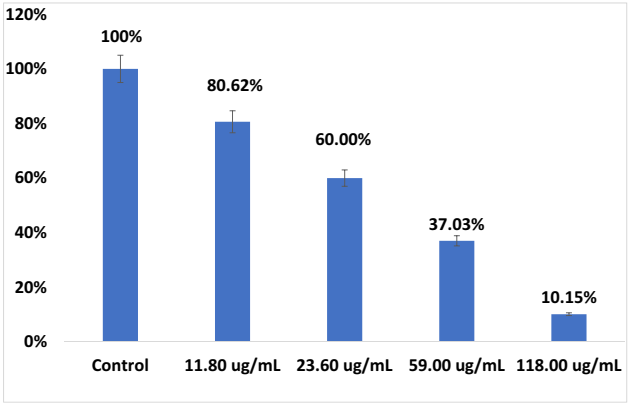

Figure 8: Cell viability analysis of HCT-116 cells by MTT assay.

The purity, crystalline nature, and size of NPs were assessed using XRD analysis. The XRD analysis revealed that the CuO NPs exhibited diffraction peaks at 2θ, namely 32.2°, 35.2°, 38.8°, 48.6°, 53.2°, 57.8°, 61.3°, and 67.8°. These peaks corresponded to the crystallographic planes (110), (002), (111), (202), (020), (202), (113) and (220), respectively (Figure 4). These findings confirm the successful green synthesis of pure and monoclinic structure of CuO NPs. The present findings align with prior studies on CuO NPs synthesized via environmentally friendly techniques [34,37,38]. The average crystallite size, as determined by the Debye–Scherer formula, was 10.88 nm. The current investigation is consistent with earlier research, which found that *Seriphidium oliverianum* produced CuO NPs with a size of 12.44 nm [38].

The shape and size of the synthesized CuO NPs were assessed using SEM and TEM (Figure 5). The CuO NPs that were synthesized exhibit a distinct spherical shape, as depicted in the SEM and TEM images presented in Figure 5(a). It was observed that the biological synthesis of CuO NPs results in the production of small spherical particles with uniform dimensions. The presence of biological ingredients in the extract demonstrates the relatively small aggregation. The CuO NPs produced from the herbal drug extract exhibited a spherical morphology, aligning with earlier research findings [37,39–41]. Furthermore, the size and shape of the manufactured CuO NPs were also observed by TEM (Figure 5b). The TEM micrographs demonstrated that the NPs had an almost spherical shape and were in the ranged of 4–20 nm (average size ~8 nm). This is similar to earlier investigations [32,40,42].

Standard broth dilution techniques were used to assess the antibacterial and antifungal activity (MIC) that were found in the range of 1–2.5 mg·mL^{-1} against tested pathogens. The study demonstrated that CuO NPs had better antibacterial efficacy against MRSA in comparison to MDR-PA and *C. albicans*. The results of MIC values align with the findings reported by Javadhesari et al. [43] in their earlier research. In a previous study an MIC value of 2.5 to 3.5 mg·mL^{-1} has been reported for *E. coli* and *S. aureus*, respectively [43]. Amiri et al. also observed a comparable

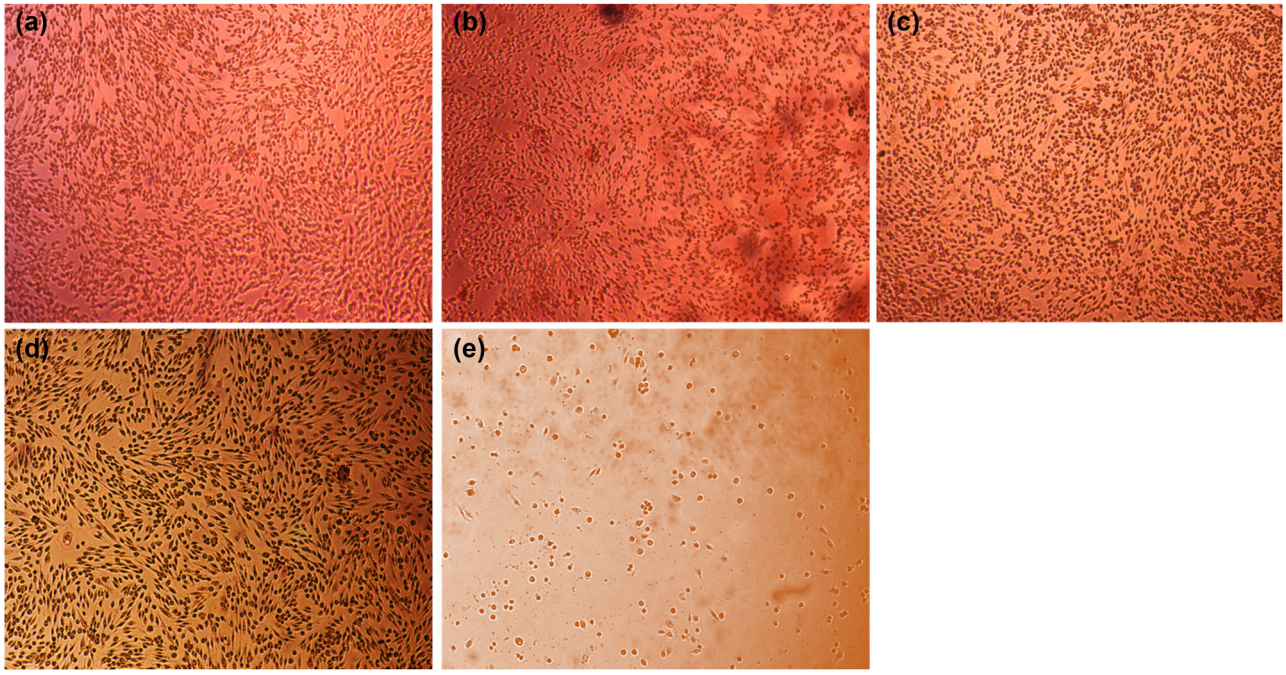

Figure 9: Microscopic analysis of the HCT-116 cells. (a) Control and (b–e) treated with 11.8, 23.6, 59, and 118 µg·mL^{-1} of NPs, respectively.

trend in the MIC of CuO NPs against *Candida* species. The MIC50 of CuO NPs against *Candida* species was reported as 1,000 μg·mL^{-1} [3,44]. The CuO NPs produced by *Solanum tuberosum* extract have been shown to have the antimicrobial activity of 0.2–1 mg·mL^{-1} [41]. Ren et al. previously documented that CuO NPs had antibacterial efficacy within the concentration range of 2,500–5,000 μg·mL^{-1} against several bacterial strains [45].

In addition, the impact of CuO NPs on the physical characteristics of MRSA, MDR-PA, and *C. albicans* was also examined by SEM (Figure 7). The control without treatment MRSA cells exhibited a smooth and intact cell surface, displaying typical, regular, and spherical morphological characteristics (Figure 7a). Nevertheless, the application of CuO NPs to MRSA cells demonstrated substantial impairment of the microorganisms and a significant decrease in their cell population. The cell wall and membrane exhibited distortions, irregularities, roughness, and lack of integrity, suggesting the loss of membrane integrity that ultimately results in cell death (Figure 7a1). Similarly, the MDR-PA cells that were not treated exhibited a healthy, normal, and rod-like architecture with a smooth cellular membrane (Figure 7b). However, when MDR-PA cells were exposed to CuO NPs, the cells exhibited severe damage. The cell membrane and wall were found to be disrupted, deformed, inconsistent, and coarse indicating a lack of cellular membrane integrity (Figure 7b1). The *C. albicans* cells that were not treated exhibited a sleek cell architecture characterized by an undamaged oval-shaped appearance (Figure 7c). The *C. albicans* cells that were subjected to CuO NPs exhibited an irregular and arbitrary cell surface, resulting in significant damage to the cells. In addition, the cells that were severely damaged were no longer in their original state, which could ultimately result in cell death (Figure 7c1). It was suggested that the Cu^{2+} ions have the potential to be easily released from CuO NPs, enabling them to interact more efficiently with membrane lipids and potentially trigger oxidation [35,36]. These interaction causes the membrane to collapse, resulting in the release of intracellular substances and enabling the interaction of CuO NPs with bacterial DNA, enzymes, and proteins [34]. Furthermore, it has been stated that the production of reactive oxygen species is responsible for CuO's antibacterial action [35,36]. These processes can diminish the potential for survival of the cells and result in cellular death.

Furthermore, inhibition of biofilm formation by CuO NPs was investigated by microtiter crystal violet assay (Figure 6). Microorganisms adhere irreversibly to surfaces to form biofilms, which are the sources of subsequent infections. CuO NPs dose-dependently decreased the biofilm formation in tested pathogens. As the concentration of CuO NPs increased, the decrease in biofilm was observed. The highest concentration of 2 mg·mL^{-1} decreased the biofilm by 92.91%, 79.84%, and 71.57% for *P. aeruginosa*, MRSA, and *C. albicans*, respectively (Figure 6). The findings of our study align well with prior research, which has demonstrated the suppression of biofilm formation through the utilization of CuO NPs. Bai et al. [46] observed a significant reduction of 90% in *S. aureus* biofilm when exposed to 1,000 μg·mL^{-1} of CuO NPs. CuO NPs were found to suppress *C. albicans* biofilm development in a dose-dependent manner and inhibit it by 75% at 500 μg·mL^{-1} [47]. LewisOscar et al. [48] also reported a 90% decrease in biofilm by copper NPs. We are also of the opinion that the reduction in cell numbers in treated samples may be due to the absence of exopolysaccharides (EPS) secretions that did not allow the microorganism to adhere to the surface. It has been reported that EPS is crucial for the persistent adhesion of microbes to a surface [49]. Additionally, the EPS layers serve as a barrier to protect the microorganisms from adverse environmental conditions [50]. Furthermore, research has indicated that biofilm inhibition by CuO NPs is might be due to the suppression of enzymes, EPS, and virulence factors [46].

To predict the probable side effects of a drug, toxicity analysis is a critical component of toxicity studies. The cytotoxicity of CuO NPs has been further examined using MTT (Figure 8) and microscopic (Figure 9) techniques. MTT assay is associated with measuring material cytotoxicity dose dependently [51]. The assay relies on the concept that viable cells possess the ability to convert the MTT dye into a purple crystalline formazan product by the action of the NAD(P)H-dependent oxidoreductase enzyme, resulting in a color change from yellow to insoluble purple. The findings demonstrated a reduction in cell viability that was directly proportional to the dosage when treated with CuO NPs. It was found that there was an 89.85% decline in cell viability at the highest concentration of NPs i.e., 118 μg·mL^{-1} (Figure 8). Furthermore, in comparison to the control, the microscopic images revealed a decrease in the number of viable cells (Figure 9). After being exposed to NPs, HCT-116 cells may experience morphological changes that are obvious signs of the NPs' cytotoxicity. The microscopic images shown in Figure 9 illustrate the apparent loss of the original shape and size of cells under the experimental treatments. The cells treated with 11.8, 23.6, 59, and 118 μg·mL^{-1} of CuO NPs notably show a considerable loss in plasma membrane and integrity of structure when compared to the control group without treatment (Figure 9). This was most likely the result of effective contact between the CuO NPs and HCT-116 cells, which increased stress and may cause cell death. It is clear that the internalization of CuO NPs via cell membrane penetration served as the

primary mechanism for cell death in HCT-116 cells due to a substantial damage of cytoplasm [52]. Our findings align with the prior research conducted by Tabrez et al. [53], which demonstrated the suppression of the HCT-116 cell line through the use of CuO NPs and found that when exposed to a concentration of 35 $\mu g \cdot mL^{-1}$, only 21% of the cells were able to survive. In addition, Gnanavel et al. [54] showed that when 100 $\mu g \cdot mL^{-1}$ of CuO NPs are applied to the HCT-116, 22% of the cells remain viable. It has already been shown that CuO NPs in the range of 100–5,000 $\mu g \cdot mL^{-1}$ did not show any cytotoxic effect on human cells [55]. In addition, CuO NPs have been utilized since the nineteenth century as a secure and efficient antibacterial agent [56]. From a cytotoxic perspective, the US Environmental Protection Agency has found that CuO NPs are safe for human usage because they are low in toxicity and environmentally safe [57,58].

7 Conclusion

NPs can also be synthesized from herbal drugs since previous reports are only regarding synthesizing CuO NPs from plants or microorganisms. The production of CuO NPs from the herbal drug septilin is described for the first time in this report. Green-synthesized CuO NPs from the drug septilin can be effectively used as antimicrobial against gram-positive, gram-negative, as well as fungus. CuO NPs also possess antibiofilm efficacy as they downregulated the biofilm formation at all concentrations tested. Furthermore, the CuO NPs also showed anticancer activity as tested on human colorectal cancer (HCT-116). The number of viable cells (HCT-116) decreased upon treatment with NPs. The present study emphasizes a new and innovative approach for generating NPs with significant potential in the field of biotechnology. This method offers a viable avenue for large-scale production of NPs using environmentally sustainable and cost-effective procedures. Hence, the produced CuO NPs have promise for future investigations in many biological and therapeutic domains, including the treatment of microbial biofilm infections, as well as the inhibition of cancer cell growth.

Acknowledgments: The authors extend their appreciation to the Deanship of Scientific Research at King Khalid University for funding this work through small Group research project under grant number (RGP1/433/44).

Funding information: This research was supported by the Deanship of Scientific Research at King Khalid University under grant number (RGP1/433/44).

Author contributions: Mohammad Azam Ansari: writing – original draft, writing – review and editing, visualization, concept, project administration; Hassan Nassr Al Dhneem, Sarah Asiri, and Firdos Alam Khan: methodology, experiments; Syed Ghazanfar Ali: writing – original draft; Yahya Fahad Jamous, Mohammad Nasser Alomary, Banan Atwah, Maryam Saleh Alhumaidi, Umme Hani, and Nazima Haider: writing – review and editing, formal analysis, visualization, revision of manuscript, resources.

Conflict of interest: Authors state no conflict of interest.

Data availability statement: The datasets generated during and/or analyzed during the current study are available from the corresponding author on reasonable request.

References

[1] Desselberger U. Emerging and re-emerging infectious diseases. J Infect. 2000;40(1):3–15.
[2] Llor C, Bjerrum L. Antimicrobial resistance: Risk associated with antibiotic overuse and initiatives to reduce the problem. Ther Adv Drug Saf. 2014;5(6):229–41.
[3] Prestinaci F, Pezzotti P, Pantosti A. Antimicrobial resistance: a global multifaceted phenomenon. Pathog Glob health. 2015;109(7):309–18.
[4] Li B, Webster TJ. Bacteria antibiotic resistance: New challenges and opportunities for implant-associated orthopedic infections. J Orthop Res. 2018;36(1):22–32.
[5] Ventola CL. The antibiotic resistance crisis: Part 1: Causes and threats. Pharm Therapeut. 2015;40(4):277.
[6] Tremblay YD, Lévesque C, Segers RP, Jacques M. Method to grow Actinobacillus pleuropneumoniaebiofilm on a biotic surface. BMC Vet Res. 2013;9(1):1–8.
[7] Koczan JM, Lenneman BR, McGrath MJ, Sundin GW. Cell surface attachment structures contribute to biofilm formation and xylem colonization by Erwinia amylovora. Appl Environ Microbiol. 2011;77(19):7031–9.
[8] Bowden GH, Li YH. Nutritional influences on biofilm development. Adv Dental Res. 1997;11(1):81–99.
[9] Dang H, Lovell CR. Microbial surface colonization and biofilm development in marine environments. Microbiol Mol Biol Rev. 2016;80(1):91–138.
[10] Røder HL, Herschend J, Russel J, Andersen MF, Madsen JS, Sørensen SJ, et al. Enhanced bacterial mutualism through an evolved biofilm phenotype. ISME J. 2018 Nov;12(11):2608–18.
[11] Juul JS, Hornung N, Andersen B, Laurberg S, Olesen F, Vedsted P. The value of using the faecal immunochemical test in general practice on patients presenting with non-alarm symptoms of colorectal cancer. Br J Cancer. 2018 Aug;119(4):471–9.
[12] Astin M, Griffin T, Neal RD, Rose P, Hamilton W. The diagnostic value of symptoms for colorectal cancer in primary care: a systematic review. Br J Gen Pract. 2011 May;61(586):e231–43.
[13] Xi Y, Xu P. Global colorectal cancer burden in 2020 and projections to 2040. Transl Oncol. 2021 Oct;14(10):101174.

[14] Zocche DM, Ramirez C, Fontao FM, Costa LD, Redal MA. Global impact of KRAS mutation patterns in FOLFOX treated metastatic colorectal cancer. Front Genet. 2015 Mar;6:116.
[15] Tuutijärvi T, Lu J, Sillanpää M, Chen G. As (V) adsorption on maghemite nanoparticles. J Hazard Mater. 2009 Jul;166(2–3):1415–20.
[16] Nalwa HS. Handbook of nanostructured materials and nanotechnology Vol 1, Synthesis and processing. United states: Academic Press; 2000.
[17] Buazar F, Sweidi S, Badri M, Kroushawi F. Biofabrication of highly pure copper oxide nanoparticles using wheat seed extract and their catalytic activity: A mechanistic approach. Green Process Synth. 2019 Jan;8(1):691–702.
[18] Sukhwal A, Jain D, Joshi A, Rawal P, Kushwaha HS. Biosynthesised silver nanoparticles using aqueous leaf extract of Tagetes patula L. and evaluation of their antifungal activity against phytopathogenic fungi. IET Nanobiotechnol. 2017 Aug;11(5):531–7.
[19] Jain D, Kour R, Bhojiya AA, Meena RH, Singh A, Mohanty SR, et al. Zinc tolerant plant growth promoting bacteria alleviates phytotoxic effects of zinc on maize through zinc immobilization. Sci Rep. 2020 Aug;10(1):13865.
[20] Ali SG, Jalal M, Ahmad H, Sharma D, Ahmad A, Umar K, et al. Green synthesis of silver nanoparticles from Camellia sinensis and its antimicrobial and antibiofilm effect against clinical isolates. Materials. 2022 Oct;15(19):6978.
[21] Ali SG, Ansari MA, Alzohairy MA, Alomary MN, AlYahya S, Jalal M, et al. Biogenic gold nanoparticles as potent antibacterial and antibiofilm nano-antibiotics against *Pseudomonas aeruginosa*. Antibiotics. 2020 Feb 27;9(3):100.
[22] Fahmy SA, Preis E, Bakowsky U, Azzazy HM. Platinum nanoparticles: Green synthesis and biomedical applications. Molecules. 2020 Oct;25(21):4981.
[23] Ali SG, Ansari MA, Jamal QM, Almatroudi A, Alzohairy MA, Alomary MN, et al. Butea monosperma seed extract mediated biosynthesis of ZnO NPs and their antibacterial, antibiofilm and antiquorum sensing potentialities. Arab J Chem. 2021 Apr;14(4):103044.
[24] Jia B, Mei Y, Cheng L, Zhou J, Zhang L. Preparation of copper nanoparticles coated cellulose films with antibacterial properties through one-step reduction. ACS Appl Mater Interfaces. 2012 Jun;4(6):2897–902.
[25] Sankar R, Manikandan P, Malarvizhi V, Fathima T, Shivashangari KS, Ravikumar V. Green synthesis of colloidal copper oxide nanoparticles using Carica papaya and its application in photocatalytic dye degradation. Spectrochim Acta Part A: Mol Biomol Spectrosc. 2014 Mar;121:746–50.
[26] Balkrishna A, Solleti SK, Singh H, Tomer M, Sharma N, Varshney A. Calcio-herbal formulation, Divya-Swasari-Ras, alleviates chronic inflammation and suppresses airway remodelling in mouse model of allergic asthma by modulating pro-inflammatory cytokine response. Biomed Pharmacother. 2020 Jun;126:110063.
[27] Khanna N, Sharma SB. Anti-inflammatory and analgesic effect of herbal preparation: Septilin. Indian J Med Sci. 2001 Apr;55(4):195–202.
[28] Naguib NI, Abd El Maguid A, Fahmy N. Radioprotective effect of septilin on radiation-induced histological and biochemical changes of rat eyes. Isotope Radiat Res. 2006;39(1):137–51.
[29] Ali SG, Ansari MA, Alzohairy MA, Alomary MN, Jalal M, AlYahya S, et al. Effect of biosynthesized ZnO nanoparticles on multi-drug resistant Pseudomonas aeruginosa. Antibiotics. 2020 May;9(5):260.
[30] Ansari MA, Govindasamy R, Begum MY, Ghazwani M, Alqahtani A, Alomary MN, et al. Bioinspired ferromagnetic CoFe2O4 nanoparticles: Potential pharmaceutical and medical applications. Nanotechnol Rev. 2023 Jul;12(1):20230575.
[31] Jalal M, Ansari MA, Shukla AK, Ali SG, Khan HM, Pal R, et al. Green synthesis and antifungal activity of Al_2O_3 NPs against fluconazole-resistant Candida spp. isolated from a tertiary care hospital. RSC Adv. 2016;109:107577–90.
[32] Garcia-Marin LE, Juarez-Moreno K, Vilchis-Nestor AR, Castro-Longoria E. Highly antifungal activity of biosynthesized copper oxide nanoparticles against Candida albicans. Nanomaterials. 2022 Nov;12(21):3856.
[33] Sukumar S, Rudrasenan A, Padmanabhan Nambiar D. Green-synthesized rice-shaped copper oxide nanoparticles using Caesalpinia bonducella seed extract and their applications. ACS Omega. 2020 Jan;5(2):1040–51.
[34] Atri A, Echabaane M, Bouzidi A, Harabi I, Soucase BM, Chaâbane RB. Green synthesis of copper oxide nanoparticles using Ephedra Alata plant extract and a study of their antifungal, antibacterial activity and photocatalytic performance under sunlight. Heliyon. 2023 Feb;9(2):e13484.
[35] Weldegebrieal GK. Photocatalytic and antibacterial activityof CuO nanoparticles biosynthesized using Verbascum thapsus leaves extract. Optik. 2020 Feb;204:164230.
[36] Ramasubbu K, Padmanabhan S, Al-Ghanim KA, Nicoletti M, Govindarajan M, Sachivkina N, et al. Green synthesis of copper oxide nanoparticles using sesbania grandiflora leaf extract and their evaluation of anti-diabetic, cytotoxic, anti-microbial, and anti-inflammatory properties in an in-vitro approach. Fermentation. 2023 Mar;9(4):332.
[37] Amin F, Khattak B, Alotaibi A, Qasim M, Ahmad I, Ullah R, et al. Green synthesis of copper oxide nanoparticles using Aerva javanica leaf extract and their characterization and investigation of in vitro antimicrobial potential and cytotoxic activities. Evid-Based Complement Altern Med. 2021 Jun;2021:5589703.
[38] Aroob S, Carabineiro SA, Taj MB, Bibi I, Raheel A, Javed T, et al. Green synthesis and photocatalytic dye degradation activity of CuO nanoparticles. Catalysts. 2023 Feb;13(3):502.
[39] Ijaz F, Shahid S, Khan SA, Ahmad W, Zaman S. Green synthesis of copper oxide nanoparticles using Abutilon indicum leaf extract: Antimicrobial, antioxidant and photocatalytic dye degradation activitie. Trop J Pharm Res. 2017 May;16(4):743–53.
[40] Nzilu DM, Madivoli ES, Makhanu DS, Wanakai SI, Kiprono GK, Kareru PG. Green synthesis of copper oxide nanoparticles and its efficiency in degradation of rifampicin antibiotic. Sci Rep. 2023 Aug;13(1):14030.
[41] Alishah H, Pourseyedi S, Ebrahimipour SY, Mahani SE, Rafiei N. Green synthesis of starch-mediated CuO nanoparticles: preparation, characterization, antimicrobial activities and in vitro MTT assay against MCF-7 cell line. Rend Lincei. 2017 Mar;28:65–71.
[42] Mali SC, Raj S, Trivedi RJ. Biosynthesis of copper oxide nanoparticles using Enicostemma axillare (Lam.) leaf extract. Biochem Biophys Rep. 2019;20:100699.
[43] Javadhesari SM, Alipour S, Mohammadnejad S, Akbarpour MR. Antibacterial activity of ultra-small copper oxide (II) nanoparticles synthesized by mechanochemical processing against S. aureus and E. coli. Mater Sci Eng: C. 2019 Dec;105:110011.
[44] Amiri M, Etemadifar Z, Daneshkazemi A, Nateghi M. Antimicrobial effect of copper oxide nanoparticles on some oral bacteria and candida species. J Dental Biomater. 2017 Mar;4(1):347.
[45] Ren G, Hu D, Cheng EW, Vargas-Reus MA, Reip P, Allaker RP. Characterisation of copper oxide nanoparticles for antimicrobial applications. Int J Antimicrob Agents. 2009 Jun;33(6):587–90.
[46] Bai B, Saranya S, Dheepaasri V, Muniasamy S, Alharbi NS, Selvaraj B, et al. Biosynthesized copper oxide nanoparticles (CuO

NPs) enhances the anti-biofilm efficacy against K. pneumoniae and S. aureus. J King Saud Univ-Sci. 2022 Aug;34(6):102120.
[47] Ansarifard E, Zareshahrabadi Z, Sarafraz N, Zomorodian K. Evaluation of antimicrobial and antibiofilm activities of copper oxide nanoparticles within soft denture liners against oral pathogens. Bioinorg Chem Appl. 2021 Jun;2021:1–7.
[48] LewisOscar F, MubarakAli D, Nithya C, Priyanka R, Gopinath V, Alharbi NS, et al. One pot synthesis and anti-biofilm potential of copper nanoparticles (CuNPs) against clinical strains of Pseudomonas aeruginosa. Biofouling. 2015 Apr;31(4):379–91.
[49] Stoodley P, Sauer K, Davies DG, Costerton JW. Biofilms as complex differentiated communities. Annu Rev Microbiology. 2002 Oct;56(1):187–209.
[50] Flemming HC, Wingerder J. The biofilm matrix. Nat Rev Microbiol. 2010;8:623–33.
[51] Gai X, Liu C, Wang G, Qin Y, Fan C, Liu J, et al. A novel method for evaluating the dynamic biocompatibility of degradable biomaterials based on real-time cell analysis. Regen Biomater. 2020;7:321–9.
[52] Almutairi HH, Parveen N, Ansari SA. Hydrothermal synthesis of multifunctional bimetallic Ag-CuO nanohybrids and their antimicrobial, antibiofilm and antiproliferative potential. Nanomaterials. 2022 Nov;12(23):4167.
[53] Tabrez S, Khan AU, Mirza AA, Suhail M, Jabir NR, Zughaibi TA, et al. Biosynthesis of copper oxide nanoparticles and its therapeutic efficacy against colon cancer. Nanotechnol Rev. 2022;11:1322–31.
[54] Gnanavel V, Palanichamy V, Roopan SM. Biosynthesis and characterization of copper oxide nanoparticles and its anticancer activity on human colon cancer cell lines (HCT-116). J Photochem Photobiol B: Biol. 2017;171:133–8.
[55] Allaker RP. The use of nanoparticles to control oral biofilm formation. J Dent Res. 2010;89:1175–86.
[56] Dollwet HHA, Sorenson JRJ. Historic uses of copper compounds in medicine. Trace Elem Med. 1985;2(2):80–7.
[57] Sankar R, Maheswari R, Karthik S, Shivashangari KS, Ravikumar V. Anticancer activitiy of Ficus religiosa engineered copper oxide nanoparticles. Mater Sci Eng C. 2014;44:234–9.
[58] Elemike EE, Onwudiwe DC, Nundkumar N, Singh M. CuO and Au-CuO nanoparticles mediated by Stigmaphyllon ovatum leaf extract and their anticancer potential. Inorg Chem Commun. 2019 Jun;104:93–7.